RSC Advances

ROYAL SOCIETY OF CHEMISTRY

www.rsc.org/advances

RSC Advances

RSCPublishing

ARTICLE

One-Step Growth of Isoreticular Luminescent Metal-Organic Frameworks on Cotton Fibers

Cite this: DOI: 10.1039/xoxxoooooox

R.R. Ozer* and J.P. Hinestroza

Received ooth November 2014,
Accepted ooth January 2015

DOI: 10.1039/xoxxoooooox

www.rsc.org/

A series of isoreticular lanthanide metal-organic frameworks, Ln-MOFs (Ln=Eu, Gd, and Tb), were directly grown on cotton fibers using a room temperature water-based direct precipitation method. This facile synthesis protocol involves equimolar concentrations of aqueous Ln^{3+} salts and 1,3,5-benzenetricarboxylic acid that enables effective crystallization of high amount of Ln-MOFs on cotton fibers. 1D thin, continuous, and dense wire-like structures were obtained. Ln-MOF structures were found well attached to the cotton fibers while maintaining their crystal structures. Under UVC exposure, intense emissions of red, blue, and green were observed for Eu-, Gd-, and Tb-MOFs. Potential applications of this technology include protective clothing, textile-based sensors, and smart tagging.

Introduction

Metal organic frameworks (MOFs) are 3D inorganic-organic porous crystalline materials built from metal ions linked by polydentate organic linkers.[1,2] Some of the most widely studied linkers used in MOFs syntheses are based on carboxylate, imidazole, and pyridyl functional groups, facilitating formation of more rigid frameworks by aggregating metal ions into M-O-C molecular units (secondary building units, SBU).[3,4] MOFs have found many potential applications including gas absorption,[5] separation,[6] catalysis,[7] and sensing[8] owing to their high porosity (>50% of their crystal volume), surface area (ranging from 1,000 to 10,000 m^2/g), facile and modular synthesis protocols, and structural diversity.

Controlled attachment of functional nanostructures to textiles is of significant importance for the development of protective clothing and smart textiles.[9] The ideal methodology would involve cost effective, room temperature, environmentally benign, one-step, and *in-situ* growth of functional nanostructures from precursors. MOFs are specifically suitable for the job; with well-defined, large, accessible cavities, and high surface area that are able to trap hazardous agents in proximity to catalytically active sites, increasing the decontamination rate.[10,11] Despite the increasing interest in MOFs in recent years, immobilization of MOFs on flexible solid supports is in its infancy. Recently, Cu-MOFs was immobilized on cotton fibers and its antibacterial activity was demonstrated.[12,13] In addition, Kusgens *et al.* showed that Cu-MOFs deposition on pulp fibers was also possible.[14] Meilikhov *et al.* deposited a thin layer of MOFs by stepwise addition of preformed Cu-MOFs on COOH-terminated polyester fibers.[15] Recently, Zhao *et al.* reported that a nanoscale coating of Al_2O_3 formed by atomic layer deposition on the surface of polypropylene, polybutylene terephthalate, and cotton fibers facilitates the growth of MOFs with high loadings.[16,17]

Electropun nanofibers can also be utilized as the platform upon which MOFs can be grown. Centrone *et al.* reported the direct growth of MIL-47 on electrospun polyacrylonitrile nanofibers by microwave irradiation.[18] Jin *et al.* demonstrated that ZIF-8 crystals grown on electrospun polyimide mats are effective catalysts for aldol condensation.[19] In a similar fashion, Lian *et al.* reported high adsorption capacity of ZIF-8 crystals grown on electrospun polyurethane nanofibers for N_2, O_2, H_2, and CO_2.[20]

Transition metal containing MOFs, such as HKUST-1 (Cu-1,3,5-benzenetricarboxylic acid) and MOF-5, (Zn-1,4-benzenedicarboxylic acid) are some of the most widely studied structures.[1–3,5–8] However, lanthanide containing coordination frameworks (Ln-MOFs) can add luminescence to MOFs' already vast toolbox of features, opening up new venues such as colorimetric sensing.[21–33] Ln-MOFs have unique optical properties such as long luminescence lifetime, large stoke shift, and sharp monochromatic emission bands.[31] Among them, complexes of Eu^{3+}, Gd^{3+}, and Tb^{3+} have been the most widely investigated due to their strong red, blue, and green emission colors and are the object of the study in this report. Eu-, Gd-, and Tb-MOFs have been shown to have identical structures (isoreticular) and physical properties.[32] Lobkovsky and collaborators have explored the change in fluorescence intensity of Eu- and Tb-MOFs upon small molecule entrapment, showing potential sensing applications.[27,28] A recent report by Guo *et al.* demonstrated that the Tb-MOFs film on glass supports can also selectively detect organic solvents.[33] Moreover, in a series of studies Qui and collaborators

demonstrated the potential of luminescent MOFs for selective sensing of organoamines.[26]

Although the luminescence mechanisms and the synthetic protocols of lanthanide-based MOFs have been well studied, they haven't been incorporated into flexible materials such as cotton fibers. Lack of visible absorption, variable UV emission upon entrapment of guest molecules, and facile room temperature synthesis techniques position Ln-MOFs as effective platform for the development of wearable technologies.[34] Herein, we detail the synthesis, characterization, and photoluminescence properties of selected trivalent lanthanide (Ln) MOFs grown on cotton fibers. Luminescent crystals were grown at room temperature by the reaction of $Eu(NO_3)_3$, $Gd(NO_3)_3$, or $Tb(NO_3)_3$ with 1,3,5-benzenetricarboxylic acid (BTC) in a mixed solvent of ethanol and water in the presence of cotton swatches at room temperature for 48h. While all the Ln-MOFs exhibited similar one-dimensional rod-like morphology ranging in diameter 3-10 micron, they behave differently upon attachment to the cotton fibers. Eu-MOFs fully wraps around the cotton fibers; whereas Gd- and Tb-MOFs form mainly short, frangible, and wire-like structures. We observed that the Ln-MOFs were durably attached onto the cotton fibers. Eu, Gd, and Tb MOFs grown on cotton fibers displayed intense red, blue, and green emissions at room temperature under UV light.

Experimental Section

Materials: Desized cotton fabric (#400) was purchased from TestFabrics, Inc (West Pittson, PA). Europium (III) nitrate pentahydrate ($Eu(NO_3)_3.5H_2O$, 99.9% trace metals basis), Gadolinium(III) nitrate hexahydrate ($Gd(NO_3)_3.6H_2O$, 99.99% trace metal basis), Terbium (III) nitrate pentahydrate ($Tb(NO_3)_3.5H_2O$) (99.9% trace metal basis), 1,3,5-benzenetricarboxylic acid ($C_6H_3(CO_2H)_3$, 95%), ethanol (ACS reagent, ≥ 99.5%), and sodium hydroxide pellets (NaOH, ACS reagent, ≥ 97.0%) were purchased from Sigma-Aldrich.

Cleaning of cotton fabric: Before the luminescent MOFs were grown, the cotton fabric was cut into square swatches (2 cm×2 cm) and scoured to remove wax, grease, and other finishing chemicals. The scouring solution was prepared by dissolving 1.0 g of NaOH in 100 mL of deionized (DI) water. In the scouring process, four cotton swatches were placed in a 250 mL round-bottom flask. The mixture was stirred at 100 °C for 1 h. At the end of the process, scoured swatches were removed from the solution, rinsed thoroughly with DI water, and dried in air. To ensure uniform growth of MOFs on cotton surfaces in subsequent steps, the swatches were fixed to a glass slide using epoxy glue (LOCTITE stik'n seal ultra, Flextec Technology, Inc). The immobilized swatches were then suspended vertically in a 21 mL growth solution.

Growth of luminescent Ln-MOFs on cotton fibers: 0.50 mmol of $Ln(NO_3)_3$ ($Eu(NO_3)_3.5H_2O$, $Gd(NO_3)_3.6H_2O$, or $Tb(NO_3)_3.5H_2O$) was dissolved in a 15 mL solvent mixture of ethanol:water (1:1 v/v). Equimolar 1,3,5-benzenetricarboxylic acid (BTC) (0.50 mmol) solution was prepared separately in a 6 mL ethanol:water (2:1 v/v) solvent mixture. Glass slides containing cotton swatches were immersed in Ln solution in a glass-staining dish that could contain 5 slides, with a ground glass cover. After incubation at room temperature for 30 min., BTC solution was added dropwise to this solution. The containers were sealed with parafilm, placed in a platform shaker (120 rpm), and incubated at room temperature for 48 h to facilitate crystal growth. At the end of the incubation time, samples were removed, washed with water and ethanol, and cured in an oven at 120 °C for 2 h. A white precipitate was observed for each Ln-MOFs at the end of the incubation cycle, which was collected by filtration, washed with DI water and ethanol, dried at 80 °C under vacuum, and analyzed separately. The products are stable in air and insoluble in water and ethanol.

Characterization: Morphology of the materials was investigated using a LEO 1550 field emission scanning electron microscope (FESEM). Crystal structures were analyzed using a Scintag X-Ray Diffractometer with Cu Kα radiation, employing a scanning rate of 0.02° s^{-1} within the range of 2θ=5°-35°, operating at 40 kV and 40 mA. Photoluminescence data were collected using Renishaw InVia Raman microscope with a laser wavelength of 488 nm. Fourier Transform Infrared (FTIR) spectroscopy was carried out in a Nicolet Magna 760 FTIR spectrometer (Thermo Fisher Scientific Inc., Waltham, MA) in single attenuated total reflectance (ATR) mode. Thermogravimetric analysis (TGA) was carried out using a TA Instruments TGA 2950. The samples were heated from 40 °C to 650 °C at a rate of 10 °C/min under a nitrogen atmosphere at a flow rate of 40 mL/min in an aluminum pan. The amount of Lanthanide MOFs grown on cotton samples was calculated by the weight loss of the samples at the end of the heating cycle. In the event, three pieces were sampled from each treated cotton swatch along with control samples of untreated cotton. Photographic images were captured using a cell phone camera. A hand held UVP™ UV lamp (6W compact, 365 nm) was used to capture images in a dark room.

Results and Discussion

The one step *in-situ* synthesis protocol of Ln-MOFs (Eu^{3+}, Gd^{3+}, and Tb^{3+}) is illustrated in Figure 1. Briefly, each Ln-MOFs were grown on cotton swatches by incubating them in an equimolar mixture of corresponding nitrate salt and 1,3,5-benzenetricarboxylic acid (BTC) in a water/ethanol (1:1 v/v) solution at room temperature for 48 h. All the Ln-MOFs in this study are isoreticular,[32] which is further evidenced by powder X-ray diffraction analyses (Figure 6). Each Ln atom is coordinated by six oxygen atoms from the carboxylate groups of BTC and further capped by one distorted water molecule. The carboxylate groups pin down each metal ion to produce rigid modules, referred to as secondary building units (SBUs).[4] These SBUs are joined together by organic linkers producing a 3D interconnected network.

RSC Advances

RSCPublishing

ARTICLE

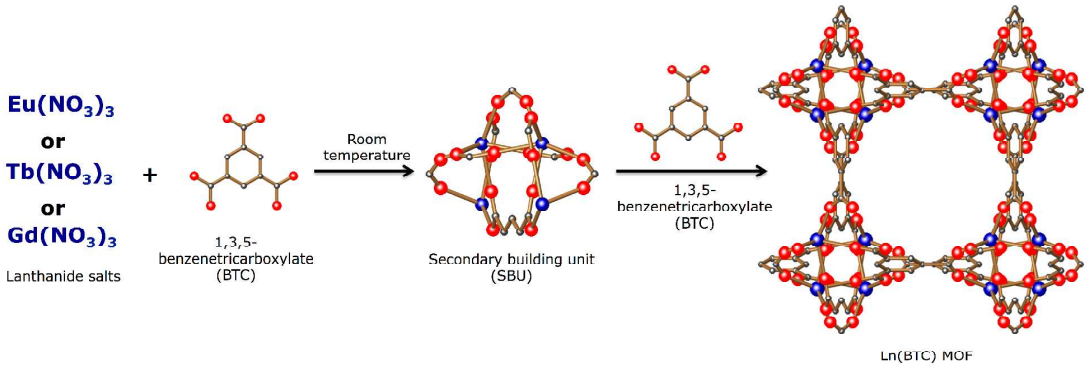

Figure 1. Schematics for the synthesis of Lanthanide metal-organic frameworks (Ln-MOFs) via copolymerization of Eu^{3+}, Gd^{3+}, or Tb^{3+} with equimolar BTC. Secondary building units (SBUs) are formed through rigid M-O-C core clusters. Subsequently, each SBU acts as a large rigid vertex linked together by the BTC to produce luminescent extended frameworks. (Lanthanides: blue; O, red; C, gray). All hydrogen atoms have been omitted for clarity. Crystal structure of $Eu(NO_3)_3.5H_2O$ as a representative of isoreticular MOFs was adopted from Ref.[27] and is available free of charge from The Cambridge Crystallographic Data Centre via www.ccdc.cam.ac.uk/conts/retrieving.html with CCDC-61749292.

Figure 2-4 depict SEM images of the Ln-MOFs grown on cotton fibers at various magnifications. After folding and stretching the cotton swatches containing luminescent MOFs, visual as well as SEM analysis didn't show a significant difference in terms of MOF contents and photoluminescence. Energy dispersive X-ray analyses reveal the presence of Eu, Gd, and Tb ions on each cotton sample (ESI). The difference in the morphology of the samples is striking. 1D thin, continuous, and flexible Eu-MOFs fully wraps around the cotton fiber (Figure 2). Individual fibrous MOFs structures are easily discernable. However, Gd- and Tb-MOFs form mainly short, frangible, and wire-like structures distributed unevenly on the surface of the cotton fibers. Dandelion-like crystals were also observed, which can also account for higher amount of both Gd- and Tb-MOFs grown on cotton samples (Table 1).

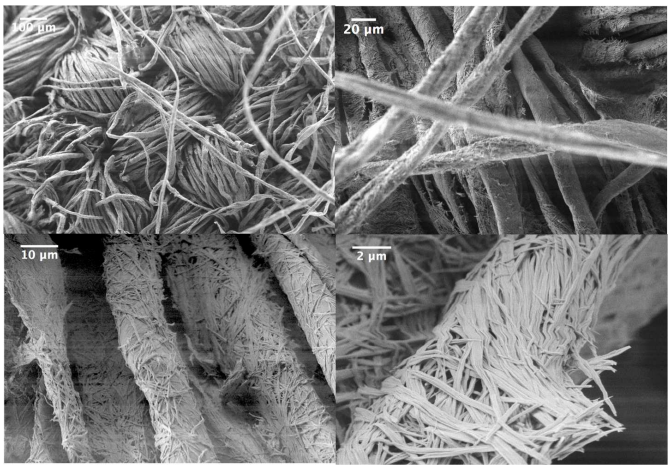

Figure 2. SEM images of the Eu-MOFs grown on cotton fibers at various magnifications.

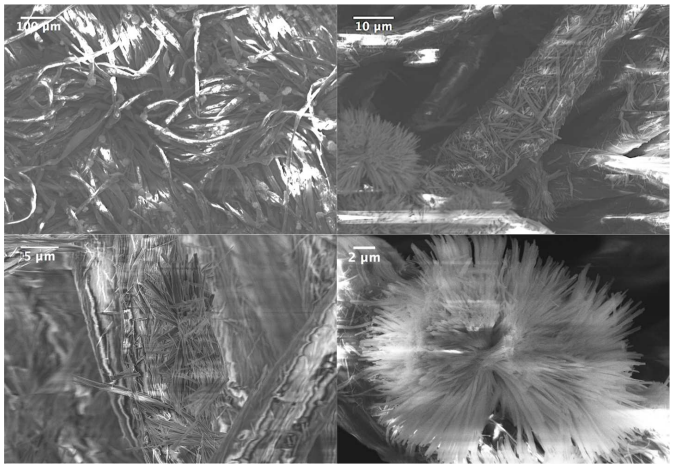

Figure 3. SEM images of the Gd-MOFs grown on cotton fibers at various magnifications.

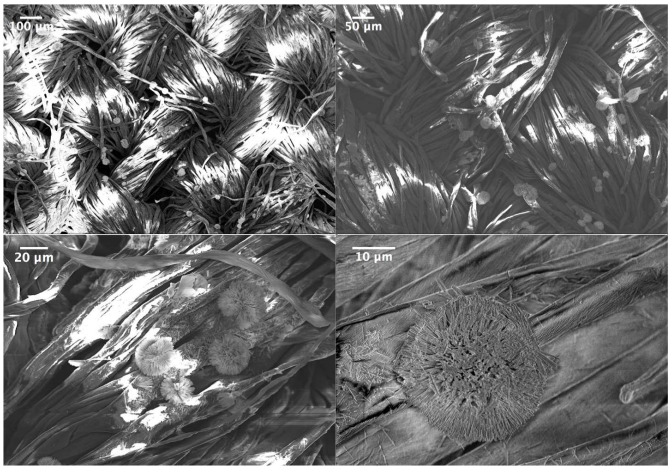

Figure 4. SEM images of the Tb-MOFs grown on cotton fibers at various magnifications.

Each white precipitate obtained at the end of incubation cycle was collected by filtration, washed with DI water and ethanol, and dried at 80 °C under vacuum (Figure 5). The products are stable in air and insoluble in water and ethanol. The powders exhibit 1D rod-like structures with lengths up to 10 micron. Particularly, the Eu-MOFs nanowires seem flexible to bending deformation. This type of anisotropic growth of the Ln-MOFs is in agreement with the previous reports.[35]

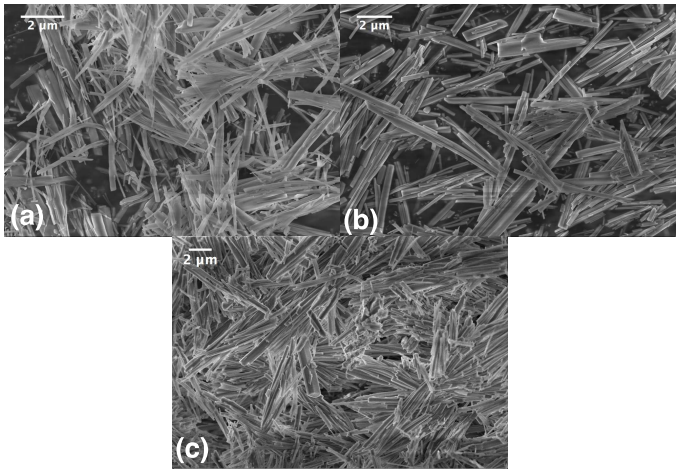

Figure 6. PXRD patterns of Ln-MOFs a) solids collected after the growth b) grown on cotton fibers.

Structures of the resulting samples were analyzed by powder X-ray diffraction (PXRD). Figure 6a demonstrates the PXRD patterns of Ln-MOFs solids which are almost identical, agreeing with he previous reports that they are isoreticular.[32,35] Figure 6b depicts PXRD patterns of Ln-MOFs grown on cotton samples. The broad peak at 2θ=22.5° is associated with the crystalline cellulose structure. The predominant peak at 2θ=17° is clearly visible in solid as well in cotton samples indicating that the basic frameworks were retained upon cotton immobilization.

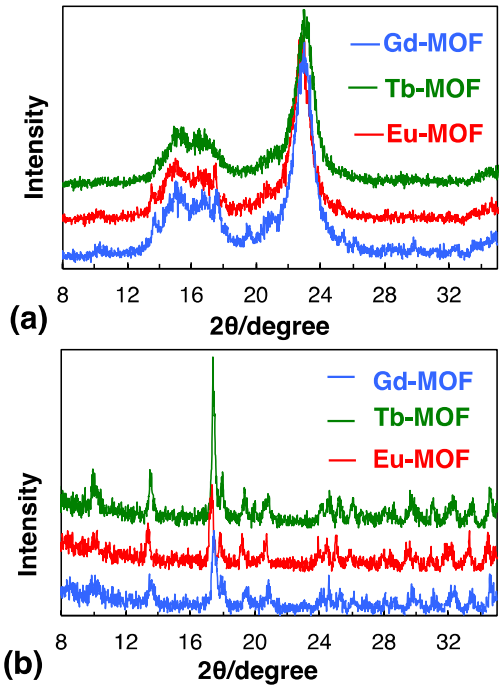

Figure 6. PXRD patterns of Ln-MOFs **(a)** solids collected after the growth **(b)** grown on cotton fibers.

To further verify Ln-MOFs formation, samples were characterized by FTIR (Figure 7 a,b). All Ln-MOFs show similar FTIR spectra, further evidence that the three MOFs are isoreticular. Free H_3BTC has absorption bands at 1692 cm^{-1} and 1280 cm^{-1} due to the stretching vibrations at higher energy and the bending vibration at lower energy of the C=O in carboxylate group (Figure 7a). Upon coordination with lanthanides, the characteristic BTC bands have similar downward shifts, suggesting that they have similar coordination structures. The bands appear at 1610–1550 cm^{-1} and 1435–1370 cm^{-1} in each Ln-MOFs, indicating coordination between carboxyl group and Ln^{3+}. The absence of a band at 1720 cm^{-1}, associated with carboxylic acid, is also an evidence of full deprotonation of H_3BTC.[35] Figure 7b indicates the spectra of Ln-MOFs grown on cotton samples with clean cotton fabric shown as control. FTIR spectrum of clean cotton sample exhibits characteristic cellulose peaks. Strong absorption bands around 1610–1550 cm^{-1}, 1435–1370 cm^{-1} and 760 cm^{-1} can be observed in the cotton samples containing Ln-MOFs, a further indication of the presence of intact Ln-MOFs on the cotton fibers.

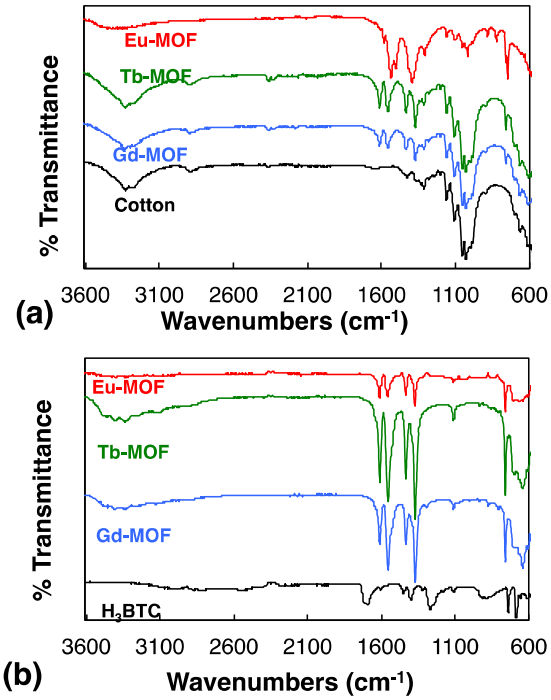

Figure 7. FTIR spectra of **(a)** H_3BTC and Ln-MOFs solids, and **(b)** clean cotton and Ln-MOFs grown on cotton fibers.

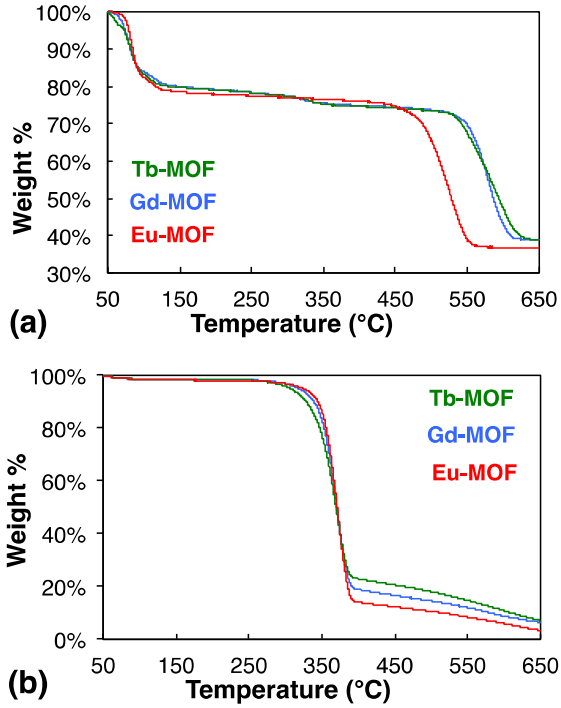

Figure 8. Thermogravimetric analyses (TGA) of **(a)** solid Ln-MOFs and **(b)** Ln-MOFs grown on cotton fibers.

Thermogravimetric analyses of solid Ln-MOFs are given in Figure 8a. The weight loss below 330 °C may originate from the loss of the absorbed water and/or ethanol molecules (approximately 20 wt%). Beyond that temperature, the weight loss is primarily assigned to the decomposition of organic moieties. Ligand decomposition starts around 450-480 °C, which is indicated by the sharp weight loss in the TGA curves, and results in formation of metal oxides around 650 °C. All solid Ln-MOFs exhibit similar thermal behavior with good thermal stability, which corroborates well with the previous work by Souza *et al*.[23] Close inspection reveals that Gd-and Tb-MOFs are much more thermally stable than Eu-MOFs, as indicated by the higher onset of the thermal decomposition (T_{onset}) values. Lanthanide's 4f electrons have a high probability of being located close to the nucleus and are thus strongly affected as the nuclear charge increases across the series (Tb>Gd>Eu). Lanthanides with higher nuclear charge form more stable complexes with oxygen-donor ligands, hence observed higher thermal stability.

TGA analyses of the cotton fabric samples containing Ln-MOFs are displayed in Figure 8b. T_{onset} for the unmodified cotton and the cotton samples with Ln-MOFs are similar within experimental error, indicating that Ln-MOFs functionalization does not alter the thermal behavior of the native cotton fibers.

TGA of solid Ln-MOFs allowed us to determine the percentage of each lanthanide in the corresponding MOFs compound. Combined with TGA curves of cotton samples containing Ln-MOFs structures, we were able to determine the extent of Ln-MOFs loading on each sample (Table 1).

Sample	T_{onset}	Weight % of Ln-MOFs grown on cotton fibers
Pristine cotton	347 °C	-
Solid Eu-MOFs	485 °C	
Eu-MOFs on cotton	351 °C	13.8 ±2
Solid Gd-MOFs	552 °C	
Gd-MOFs cotton	347 °C	15.4±2
Solid Tb-MOFs	537 °C	
Tb-MOFs cotton	341 °C	18.3±2

Table 1. T_{onset} values of the samples and the weight percentage of each Ln-MOFs grown on cotton fibers.

Figure 9 shows optical images of the solid Ln-MOFs and cotton samples containing *in-situ* grown Eu-MOFs, Gd-MOFs, and Tb-MOFs under UV light with their characteristic strong red, blue, and green emissions, respectively. Lanthanide's absorption efficiency is considerably weak with molar absorption coefficients smaller than 10 $Lmol^{-1}cm^{-1}$, resulting in a poor direct 4f excitation and hence luminescence intensity. Ligated to aromatic organic ligands with intense absorption bands,

excitation of lanthanide's 4f electrons can be stimulated through ligand-to-metal energy transfer, known as the "antenna effect". The color scheme of the solid Ln-MOFs matches those of grown on cotton fibers, supporting the XRD and FTIR observation that the 3D structures remain intact on the fiber surface.

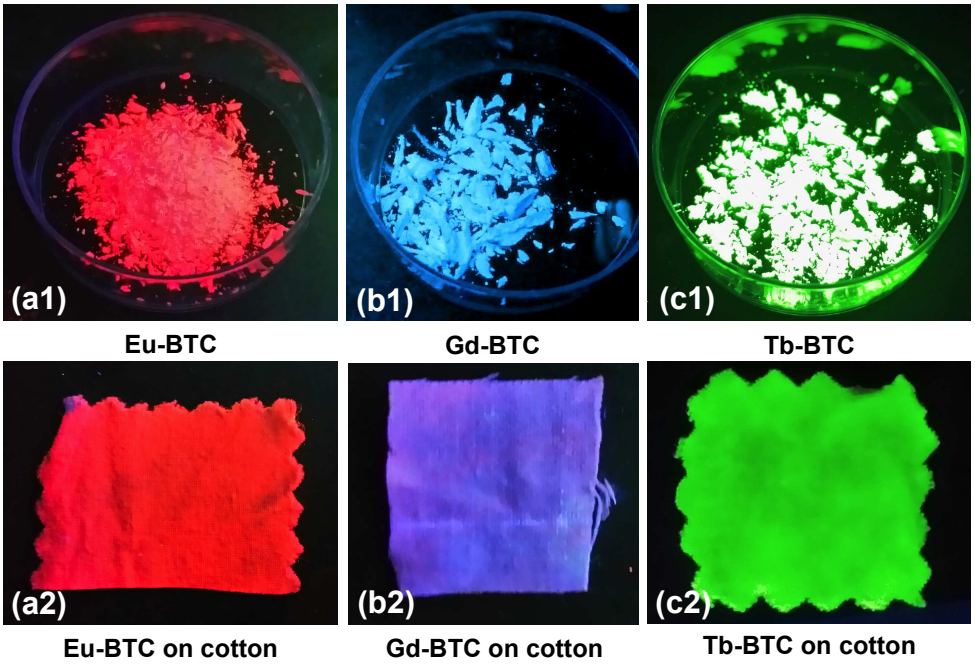

Figure 9. Intense photoluminescence of red, blue, and green **(a1)** solid Eu-MOFs, **(b1)** solid Gd-MOFs, and **(c1)** solid Tb-MOFs, and **(a2)** Eu-MOFs on cotton, **(b2)** Gd-MOFs on cotton, **(c2)** Tb-MOFs on cotton, are observed under UV illumination (λ=365 nm).

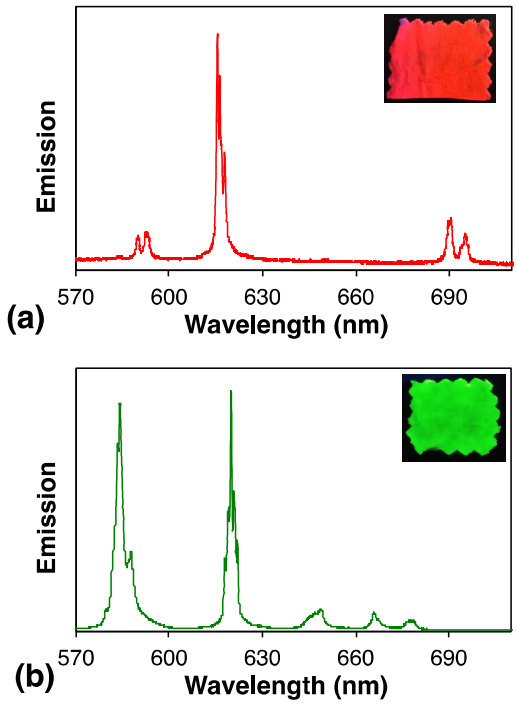

Figure 10. Photoluminescence spectra of **(a)** Eu-MOFs and **(b)** Tb-MOFs grown on cotton fibers. Inset: Photographs of Eu-MOFs and Tb-MOFs functionalized cotton samples under UV light.

Photoluminescence spectra of Eu-MOFs and Tb-MOFs in the spectral range of 530-730 nm with excitation at 488 nm are presented in Figure 10 a-b. Characteristic emission bands of Eu-MOFs were observed at 590, 614, and 690 nm with strong red emission color that are in good agreement with the previous reports.[36] The 490, 545, 587, and 621 nm emission bands are assigned to characteristic luminescence of Tb-MOFs, with a strong green emission.[23] BTC ligand acts as a luminescent sensitizer and intramolecular energy donor for these lanthanide ions, leading to a strong red and green emissions, respectively.[23] Sharp emission peaks are indicative of efficient ligand-to-metal energy-transfer mechanism. With a very large energy gap between the ground state and the first excited state, Gd(III) ion can not accept any energy from BTC ligand via intramolecular ligand-to-metal energy-transfer mechanism.[37] At 488 nm excitation, Gd-MOFs exhibit only broad-band emission which is not shown here.

Conclusions

We report on the *in-situ* growth of a series of luminescent Ln-MOFs on cotton fibers via a room temperature water-based direct precipitation technique. This facile method provides 13.8±2, 15.4±2, and 18.3±2 wt% of Eu-, Gd-, and Tb-MOFs on cotton samples, respectively. Under UV excitation, the samples display intense red, green, and blue emission colors. Upon immobilization, Ln-MOFs retain their structural integrity

and functionality. The present work demonstrates a versatile methodology that can be applied in coating any flexible substrate including polymer fibers, sheets, films, etc. A variety of molecules can be selectively detected colorimetrically by virtue of the reversible storage and release of guest molecules from the porous Ln-MOFs structures, which can be readily transformed into an external luminescence intensity change. By combining the remarkable properties of MOFs with flexible and wearable substrates, commercial applications of MOFs in fields such as filtration, chemical protective coatings, smart tagging, and catalysis can be envisioned.

Acknowledgments

We would like to thank Prof. Kay Obendorf, Cornell University Department of Fiber Science, and CIFFI for financial support. Special thanks to Mick Thomas (FESEM), Christopher Cutler Umbach (PL), and Maura Weathers (XRD) for their technical assistance. This work made use of the electronic microscopy facility of the Cornell Center for Materials Research (CCMR) with support from the National Science Foundation Materials Research Science and Engineering Centers (MRSEC) program (DMR 1120296).

Notes and references

Cornell University, College of Human Ecology, Department of Fiber Science, Ithaca, New York, 14850, US.
Electronic Supplementary Information (ESI) available: EDX Patterns and additional experimental images. See DOI: 10.1039/b000000x/

1. N. Stock and S. Biswas, *Chem. Rev.*, 2011, **112**, 933–969.
2. H. Furukawa, K. Cordova, M. O'Keeffe and O. Yaghi, *Science*, 2013, **341**, 974–986.
3. M. Eddaoudi, D. B. Moler, H. Li, B. Chen, T. M. Reineke, M. O'Keeffe and O. M. Yaghi, *Acc. Chem. Res.*, 2001, **34**, 319–330.
4. N. Rosi, J. Kim, M. Eddaoudi, B. Chen, M. O'Keeffe and O. M. Yaghi, *J. Am. Chem. Soc.*, 2005, **127**, 1504–1518.
5. J.-R. Li, R. J. Kuppler and H.-C. Zhou, *Chem. Soc. Rev.*, 2009, **38**, 1477–504.
6. S. Qiu, M. Xue and G. Zhu, *Chem. Soc. Rev.*, 2014, **43**, 6116–6140.
7. P. Valvekens, F. Vermoortele and D. De Vos, *Catal. Sci. Technol.*, 2013, **100**, 1435–1445.
8. L. E. Kreno, K. Leong, O. K. Farha, M. Allendorf, R. P. Van Duyne and J. T. Hupp, *Chem. Rev.*, 2012, **112**, 1105–1125.
9. T. Athauda, P. Hari and R. R. Ozer, *ACS Appl. Mater. Interfaces*, 2013, **5**, 6237–6246.
10. I. Ahmed and S. H. Jhung, *Mater. Today*, 2014, **17**, 136–146.
11. J. B. DeCoste and G. W. Peterson, *Chem. Rev.*, 2014, **114**, 5695–5727.
12. M. da S. Pinto, C. A. Sierra-Avila and J. P. Hinestroza, *Cellulose*, 2012, **19**, 1771–1779.
13. H. S. Rodríguez, J. P. Hinestroza, C. Ochoa-Puentes, C. A. Sierra and C. Y. Soto, *J. Appl. Polym. Sci.*, 2014, **131**, 40815–40819.
14. P. Küsgens, S. Siegle and S. Kaskel, *Adv. Eng. Mater.*, 2009, **11**, 93–95.
15. M. Meilikhov, K. Yusenko, E. Schollmeyer, C. Mayer, H.-J. Buschmann and R. A. Fischer, *Dalt. Trans.*, 2011, **40**, 4838–4841.
16. J. Zhao, M. D. Losego, P. C. Lemaire, P. S. Williams, B. Gong, S. E. Atanasov, T. M. Blevins, C. J. Oldham, H. J. Walls, S. D. Shepherd, M. a. Browe, G. W. Peterson and G. N. Parsons, *Adv. Mater. Interfaces*, 2014, **1**, DOI: 10.1002/admi.201400040.
17. J. Zhao, B. Gong, W. T. Nunn, P. C. Lemaire, E. C. Stevens, F. I. Sidi, P. S. Williams, C. J. Oldham, H. J. Walls, S. D. Shepherd, M. a Browe, G. W. Peterson, M. D. Losego and G. N. Parsons, *J. Mater. Chem. A*, 2015, **3**, 1458–1464.
18. A. Centrone, Y. Yang, S. Speakman, L. Bromberg, G. C. Rutledge and T. A. Hatton, *J. Am. Chem. Soc.*, 2010, **132**, 15687–15691.
19. R. Jin, Z. Bian, J. Li, M. Ding and L. Gao, *Dalt. Trans.*, 2013, **42**, 3936–3940.
20. Z. Lian, L. Huimin and O. Zhaofei, *Dalt. Trans.*, 2014, **43**, 6684–6688.
21. L. V. Meyer, F. Schönfeld and K. Müller-Buschbaum, *Chem. Commun.*, 2014, **50**, 8093–8108.
22. M. D. Allendorf, C. A. Bauer, R. K. Bhakta and R. J. T. Houk, *Chem. Soc. Rev.*, 2009, **38**, 1330–1352.
23. E. R. Souza, I. G. N. Silva, E. E. S. Teotonio, M. C. F. C. Felinto and H. F. Brito, *J. Lumin.*, 2010, **130**, 283–291.
24. H. Guo, Y. Zhu, S. Qiu, J. A. Lercher and H. Zhang, *Adv. Mater.*, 2010, **22**, 4190–4192.
25. D. Cai, H. Guo, L. Wen and C. Liu, *CrystEngComm*, 2013, **15**, 6702–6708.
26. S.-M. Hu, H.-L. Niu, L.-G. Qiu, Y.-P. Yuan, X. Jiang, A.-J. Xie, Y.-H. Shen and J.-F. Zhu, *Inorg. Chem. Commun.*, 2012, **17**, 147–150.
27. B. Chen, Y. Yang, F. Zapata, G. Lin, G. Qian and E. B. Lobkovsky, *Adv. Mater.*, 2007, **19**, 1693–1696.
28. B. Chen, L. Wang, F. Zapata, G. Qian and E. B. Lobkovsky, *J. Am. Chem. Soc.*, 2008, **130**, 6718–6719.
29. S. Dang, E. Ma, Z.-M. Sun and H. Zhang, *J. Mater. Chem.*, 2012, **22**, 16920–16926.
30. T. M. Reineke, M. Eddaoudi, M. O'Keeffe and O. M. Yaghi, *Angew. Chem. Int. Ed. Engl.*, 1999, **38**, 2590–2594.
31. Y. Cui, B. Chen and G. Qian, *Coord. Chem. Rev.*, 2014, **273-274**, 76–86.
32. T. M. Reineke, M. Eddaoudi, M. Fehr, D. Kelley and O. M. Yaghi, *J. Am. Chem. Soc.*, 1999, **121**, 1651–1657.
33. H. Guo, S. Zhu, D. Cai and C. Liu, *Inorg. Chem. Commun.*, 2014, **41**, 29–32.
34. K. Cherenack and L. Van Pieterson, *J. Appl. Phys.*, 2012, **112**, 091301.
35. F. Wang, K. Deng, G. Wu, H. Liao, H. Liao, L. Zhang, S. Lan, J. Zhang, X. Song and L. Wen, *J. Inorg. Organomet. Polym. Mater.*, 2011, **22**, 680–685.
36. A. V. S. Lourenço, C. A. Kodaira, E. R. Souza, M. C. F. C. Felinto, O. L. Malta and H. F. Brito, *Opt. Mater.*, 2011, **33**, 1548–1552.
37. L. F. Marques, A. A. B. Júnior, S. J. L. Ribeiro, F. M. Scaldini and F. C. Machado, *Opt. Mater.*, 2013, **35**, 2357–2365.

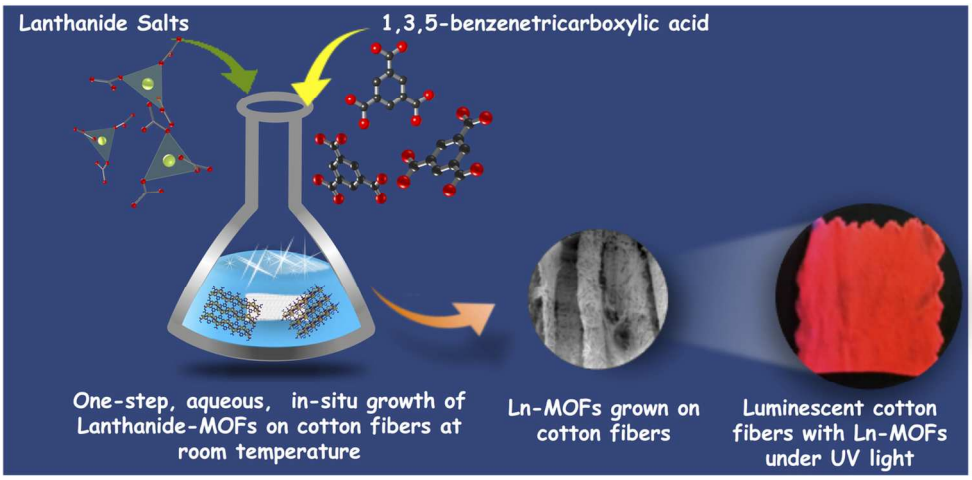

127x60mm (300 x 300 DPI)